

## 17.1 SIMULTANEOUS MEASUREMENTS OF HEAVY RAIN USING S-BAND AND C-BAND POLARIMETRIC RADARS

Alexander Ryzhkov, Pengfei Zhang, and John Krause

Cooperative Institute for Mesoscale Meteorological Studies, Norman, Oklahoma

### 1. INTRODUCTION

Rainfall measurements have been regularly performed with the first operational polarimetric WSR-88D radar (KOUN) during its system and operational tests in central Oklahoma since May 2010. Several rain events have been observed simultaneously by the S-band KOUN radar and closely located C-band dual-polarization radar (OU-PRIME) belonging to the University of Oklahoma (Palmer et al. 2011). An extensive network of rain gages is utilized for validation of radar rainfall products obtained from the two radars.

In this paper, a brief summary of validation results for S-band conventional and polarimetric QPE is presented. An extreme flash flood event in the Oklahoma City metropolitan area on 06/14/2010 has been selected for a comparative analysis of simultaneous S-band and C-band radar measurements and the results of such comparison are discussed herein. Finally, suggestions for further improvement of the radar QPE products are being made.

### 2. VALIDATION OF POLARIMETRIC QPE AT S BAND

The quality of polarimetric QPE products has been evaluated for all significant rain events during the period from May 2010 till May 2011 using the data from the KOUN WSR-88D radar and 205 gages available in Oklahoma. The performance of different versions of DP QPE algorithm has been evaluated during this study including the default DP algorithm which is currently implemented in operational polarimetric WSR-88Ds. The validation has been performed at ranges less than 120 km from the radar where contamination from frozen and mixed-phase

hydrometeors is minimal. Only storm total rain accumulations have been examined so far.

Ground truth includes the data collected by the Oklahoma Mesonet gages and micronet gages comprising three dense networks: Oklahoma City Micronet (35 gages), Agricultural Research Service (ARS) Micronet (20 gages), and Fort Cobb Micronet (16 gages). Map of gage locations is presented in Fig. 1. All three micronets are within the 120 km radius area and the total of number of gages within this area is 112.

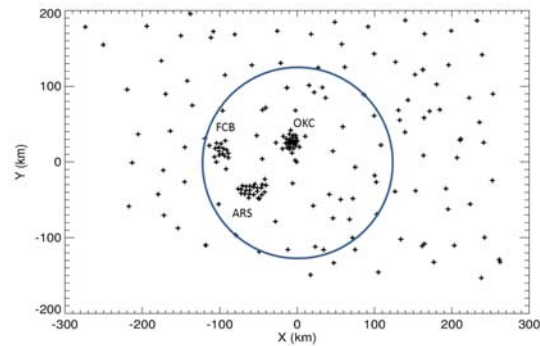


Fig. 1. Map of gage locations with respect to the KOUN WSR-88D radar. The circle corresponds to the distance of 120 km from KOUN. Three micronets are marked as OKC, ARS, and FCB.

Thirteen significant rain events have been identified for validation. A list of events is presented in Table 1.

In Table 1,  $\langle G \rangle$  means average storm rain total measured by gages and  $\max(G)$  stands for maximal gage accumulation within the radius of 120 km for a particular event. FB and FRMSE denote fractional bias and fractional RMS error of the storm total radar estimates.

Conventional algorithm for rainfall estimation implies the use of relation

\*Corresponding author address: Alexander Ryzhkov, CIMMS, University of Oklahoma, Norman, OK 73072; e-mail: Alexander.Ryzhove@noaa.gov

$$R(Z) = 1.7010^{-2} 10^{0.0714Z(\text{dBZ})} \quad (1)$$

with radar reflectivity Z capped at 53 dBZ. Several polarimetric algorithms for rainfall estimation have been tested using the dataset. The one that demonstrates most robust

performance for a whole dataset utilizes Z and specific differential phase  $K_{DP}$ :

$$\begin{aligned} R(Z, K_{DP}) &= R(Z) \quad \text{if } Z < 40 \text{ dBZ} \\ R(Z, K_{DP}) &= 44.0 |K_{DP}|^{0.822} \text{sign}(K_{DP}) \quad \text{if } Z > 40 \text{ dBZ} \end{aligned} \quad (2)$$

Table 1. Comparative performance of the conventional (R(Z)) and the best polarimetric algorithm (R(Z,  $K_{DP}$ )) for the validation dataset.

	Date	Observation period (hr)	<G> (mm)	Max (G) (mm)	FB (%)		FRMSE (%)	
					R(Z)	R(Z, $K_{DP}$ )	R(Z)	R(Z, $K_{DP}$ )
1	May 19, 2010	8	7.0	70.4	-22	-19	74	64
2	May 31, 2010	24	34.4	80.7	0	6	37	31
3	June 14, 2010	24	62.1	221.0	-28	-14	41	29
4	June 15, 2010	17	27.5	51.1	-30	-26	38	34
5	July 5, 2010	13	24.8	110.1	-52	-44	82	67
6	July 6 -7, 2010	10	20.6	79.4	-32	-25	63	57
7	July 8 - 9, 2010	13	14.8	90.2	-47	-31	111	94
8	Aug 17, 2010	24	3.6	37.4	-18	-10	78	60
9	Sept 24, 2010	24	3.8	29.8	-38	-39	80	82
10	Oct 11, 2010	6	4.3	21.0	2	1	67	62
11	Apr 23, 2011	24	7.8	76.0	57	17	129	62
12	Apr 24, 2011	24	30.9	96.4	16	-11	59	36
13	May 20, 2011	24	60.0	121.4	10	-4	27	16

The comparison between gage and radar estimates has been made provided that the magnitude of the cross-correlation coefficient  $\rho_{hv}$  exceeds 0.95. This efficiently filters out contamination from nonrain echo (such as ground clutter or biota) for both algorithms (1) and (2). Utilization of condition  $\rho_{hv} > 0.95$  improves the performance of relation (1) compared to the standard “legacy” algorithm that does not utilize polarimetric information at all.

Primary results of our analysis are contained in Table 1 and illustrated in Figs. 2 and 3 where the fractional biases and RMS errors for conventional and polarimetric algorithms are plotted for all 13 rain events.

It is evident that the polarimetric algorithm *outperforms the conventional one in terms of bias and standard error for all significant rain events* since the deployment of polarimetric prototype of the WSR-88D radar in central Oklahoma. The two algorithms perform similarly

for the event #9 (Sept 24, 2010) for which average storm total was less than 4 mm.

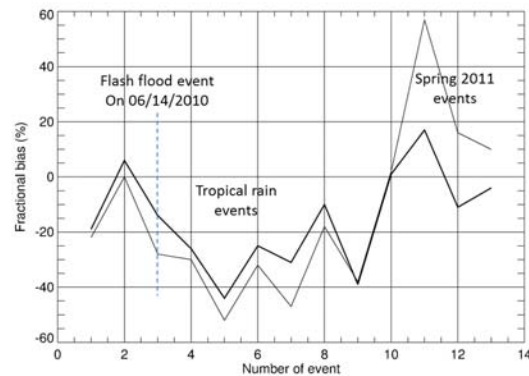


Fig. 2. Fractional biases of the storm rain total radar estimate for 13 significant rain events listed in Table 1. Thin and solid lines depict results for conventional and best polarimetric algorithms respectively.

In full agreement with previous NSSL studies (including JPOLE), the improvement via using polarimetric algorithm is most dramatic for springtime continental-type storms possibly

containing hail for which the R(Z) algorithm overestimates rain. Both conventional and polarimetric algorithms tend to underestimate precipitation in tropical-type rain which dominated rain pattern in June and July 2010. Nevertheless, such an underestimation is less pronounced if the polarimetric algorithm is used (Fig. 2). In the case of extreme flash flood in Oklahoma City on 06/14/2010, the negative bias was reduced by the factor of 2 using DP QPE. The corresponding fractional standard error (FRMSE) is diminished by more than 40%.

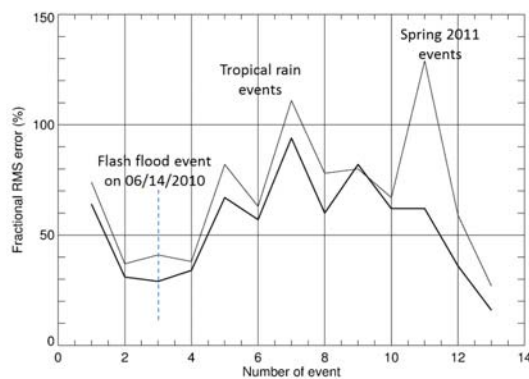


Fig. 3. Fractional RMS errors of the storm rain total radar estimate for 13 significant rain events listed in Table 1. Thin and solid lines depict results for conventional and best polarimetric algorithms respectively.

The most robust polarimetric algorithm does not utilize differential reflectivity  $Z_{DR}$  and, therefore, is immune to miscalibration of  $Z_{DR}$ . However,  $Z_{DR}$  shouldn't be counted off for DP QPE. The combination of  $Z$  and  $Z_{DR}$  may work better than the  $R(Z, K_{DP})$  relation, especially for tropical rain, but there is apparently no "universal"  $R(Z, Z_{DR})$  relation which performs equally well for all rain types.

### 3. COMPARISON OF S-BAND AND C-BAND POLARIMETRIC RADAR DATA IN THE EXTREME FLASH FLOOD CASE

A flash flood rain event in the Oklahoma City Metro area on 06/14/2010 simultaneously observed by the S-band and C-band polarimetric radars provided unique opportunity to test various types of the rainfall estimation

algorithms for a high-impact weather phenomenon. The storm quickly dumped 10 – 12 inches of rain in what would become a 500-year event at the 6- and 12-hour intervals. Widespread flooding was reported across Oklahoma City with many residents needing rescue by emergency personnel due to rising floodwaters. Ground validation of rainfall measurements in a relatively compact flash flood area has been performed using dense network of 38 rain gages, 34 of which belong to the Oklahoma City Micronet and other 4 gages constitute part of the Oklahoma Mesonet network.

Typical composite PPIs of  $Z$ ,  $Z_{DR}$ ,  $\Phi_{DP}$ , and  $\rho_{hv}$  measured at S and C bands for the flash flood case on 06/14/2010 are shown in Figs. 4 and 5. Locations of rain gages are marked by cross signs in Fig. 4.

It is evident that most of the storm precipitation is characterized by high  $Z$  associated with relatively low  $Z_{DR}$  barely exceeding 1 dB which is typical for tropical rain with high concentration of small drops. Notable is a thin line of precipitation where both  $Z$  and  $Z_{DR}$  are very high and the corresponding type of precipitation and drop size distribution is dramatically different from the ones in surrounding area. This thin line of vigorous convection apparently produces raindrops of very large size which are primarily responsible for strong attenuation and differential attenuation at C band as Fig 5 shows. Comparison of  $Z$  and  $Z_{DR}$  fields at S and C bands indicates that C-band  $Z$  is biased by about 10 dB and  $Z_{DR}$  has negative bias exceeding 6 dB in the northern direction. Applying simple linear attenuation correction based on the use of differential phase

$$\Delta Z = 0.08 \Phi_{DP} \quad \text{and} \quad \Delta Z_{DR} = 0.02 \Phi_{DP} \quad (3)$$

helps to reduce the errors in  $Z$  but is not sufficient to completely unbias  $Z_{DR}$  in northern direction where anomalously high differential attenuation occurs (Fig. 6). More sophisticated attenuation correction techniques were applied

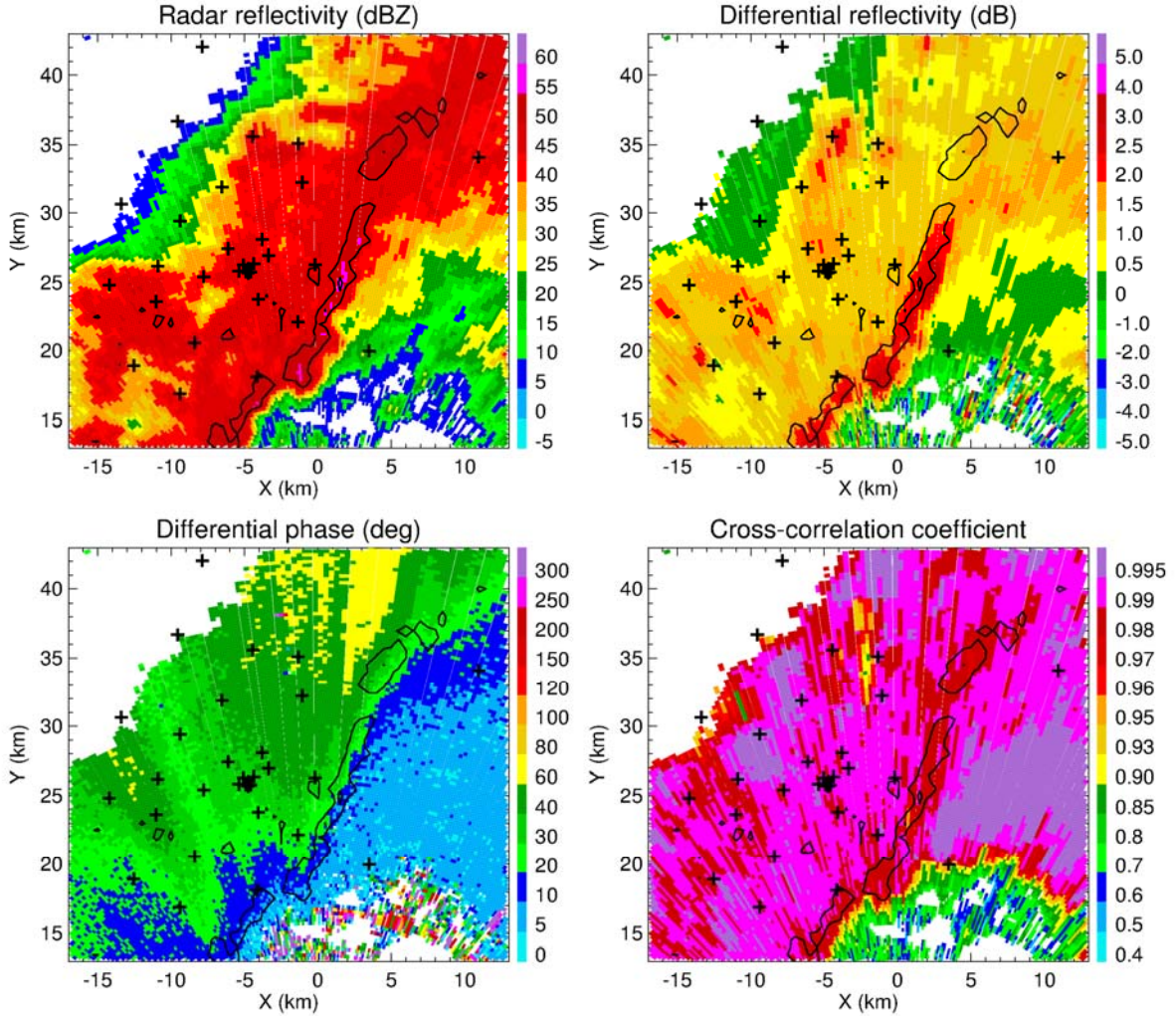


Fig. 4. Composite plot of  $Z$ ,  $Z_{DR}$ ,  $\Phi_{DP}$ , and  $\rho_{hv}$  measured by the polarimetric WSR-88D radar on 06/14/2010 in the flash flood area in Oklahoma City.  $EI = 1.4^\circ$ , 1202 UTC. Cross signs indicate locations of rain gauges.

to the C-band data in this case in a companion study of Gu et al. (2011).

Rain rates for this case were estimated using relations (1) and (2) at S band and similar relations at C band after radar reflectivity factor at C band was corrected for attenuation using Eq (3). The  $R(K_{DP})$  relation at C band has the form

$$R(K_{DP}) = 25.1 |K_{DP}|^{0.777} \text{sign}(K_{DP}) \quad (4)$$

and is applied if  $R(Z) > 5$  mm/h.

The fields of rain rates obtained using algorithms (2) at S and C bands are illustrated in Figs. 7

and 8. It is evident that the conventional  $R(Z)$  algorithm yields lower rain rates compared to the synthetic polarimetric relations except the convective line at C band. It is interesting that  $R(Z)$  at C band yields higher rain rate in the convective line as compared to  $R(Z)$  at S band due to resonance scattering effects by very large raindrops. Both  $R(Z)$  and  $R(K_{DP})$  underestimate rain in the area most affected by anomalous attenuation in the northern sector as comparison with corresponding fields at S band shows. This further emphasizes the need to utilize a more sophisticated scheme for attenuation / differential attenuation correction in the presence of "hotspots" at C band (Gu et al. 2011).

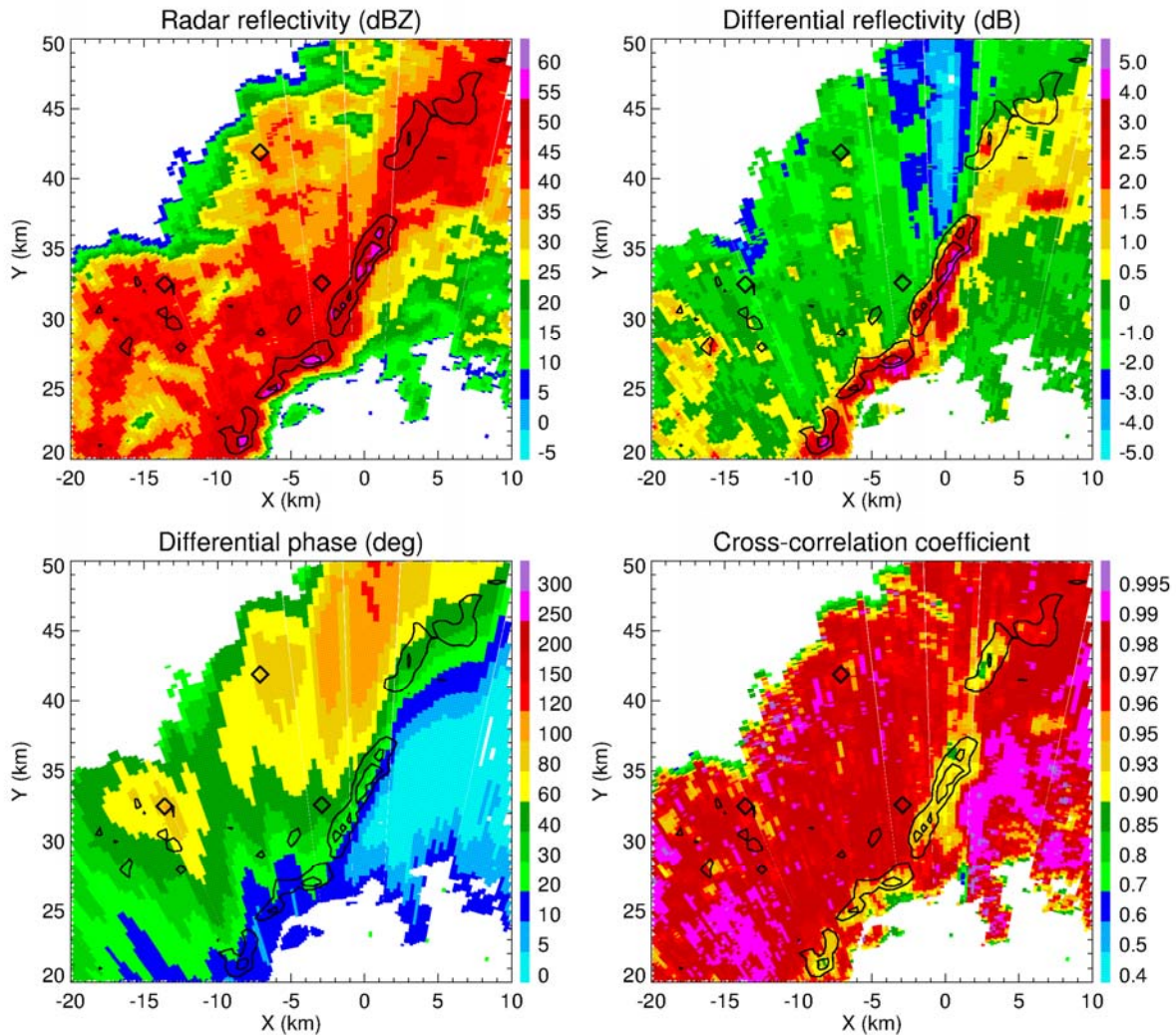


Fig. 5. Composite plot of  $Z$ ,  $Z_{DR}$ ,  $\Phi_{DP}$ , and  $\rho_{hv}$  measured by the polarimetric OU PRIME radar on 06/14/2010 in the flash flood area in Oklahoma City.  $EI = 1.5^\circ$ , 1202 UTC.  $Z$  and  $Z_{DR}$  are not corrected for attenuation.

As Table 1 and Fig. 2 show, conventional  $R(Z)$  relation (1) generally underestimates rain at S band for the 06/14/2010 event due to its “tropical” nature. The negative bias is reduced if the composite polarimetric algorithm (2) is utilized. This is further illustrated by Figs. 9 and 10 where the scatterplots of 3-hour rain accumulations (from 11 UTC till 14 UTC) obtained from the OKC Micronet gages and KOUN radar are shown for the  $R(Z)$  and  $R(Z, K_{DP})$  relations.

Despite obvious shortcomings of the simple linear attenuation correction scheme (3) in the

areas of anomalously high attenuation / differential attenuation in “hotspots”, the overall QPE improvement due to utilization of polarimetric rainfall algorithm at C band is clearly evident. The performance of the  $R(Z)$  algorithm is dramatically improved after  $Z$  is corrected for attenuation using differential phase (Fig. 11). In Fig. 11, 3-hour rain totals during the period of the most intense rain (from 1100 UTC till 0200 UTC on 06/14/2010) measured by gages are plotted versus their radar estimates using  $R(Z)$  before and after polarimetric attenuation correction (top and bottom panels, respectively).

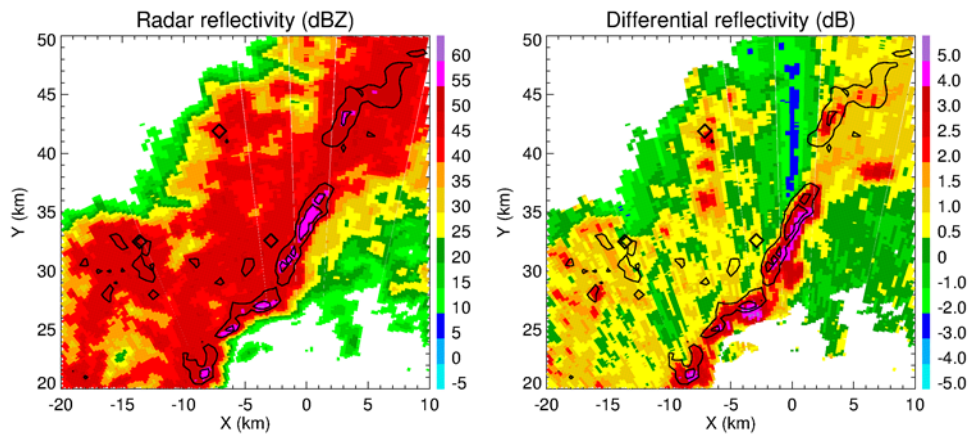


Fig. 6. The C-band fields of  $Z$  and  $Z_{DR}$  after linear polarimetric correction for attenuation is performed using Eq. (3).

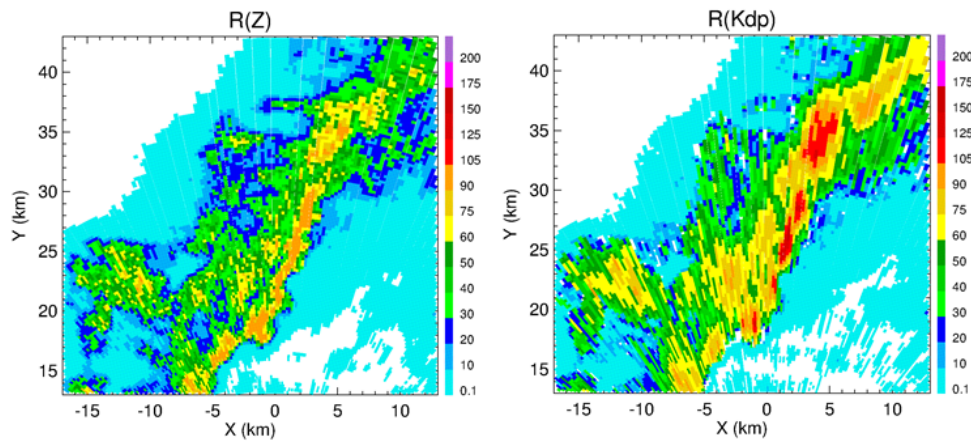


Fig. 7. Fields of rain rates obtained from the  $R(Z)$  and  $R(Z, K_{DP})$  estimates as prescribed by Eqs. (1) and (2) at S band.

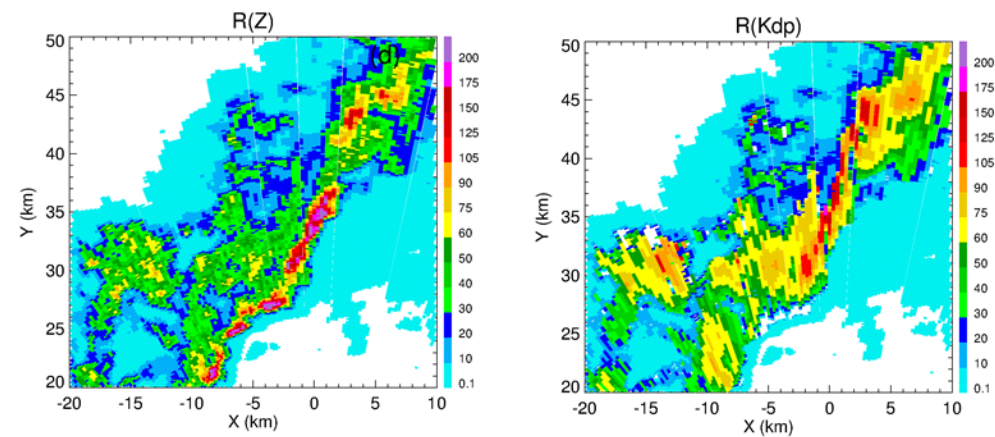


Fig. 8. Fields of rain rates obtained from  $R(Z)$  and  $R(Z, K_{DP})$  as prescribed by Eqs. (1) and (3) at C band.

Further improvement is achieved if the “synthetic” polarimetric algorithm is applied (Fig.

12). Quantitative measures of the quality of 3-hour rain total estimates by three different

methods utilizing the OU PRIME data are presented in Table 2.

coefficient between gage and radar measurements.

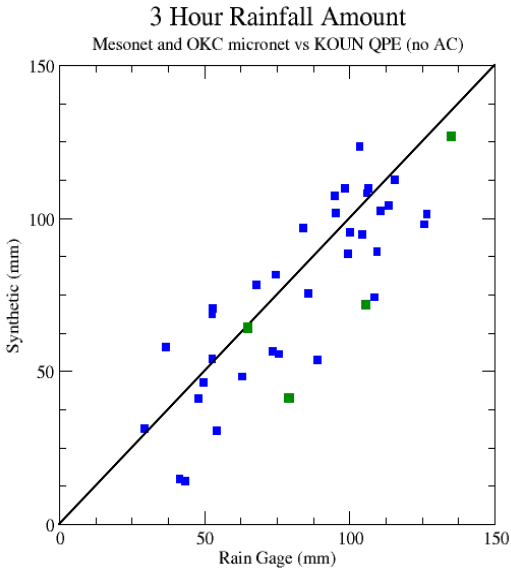
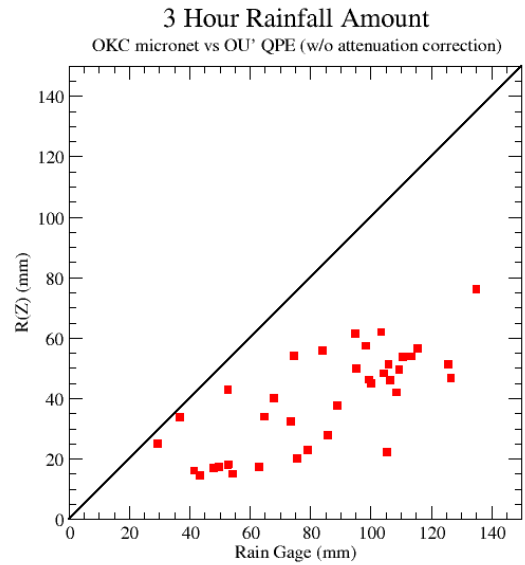


Fig. 9. Scatterplot of 3-hour rain totals measured by gages versus their radar estimates using S-band data and the  $R(Z)$  relation (1).



3 Hour Rainfall Amount  
OKC micronet vs OU<sup>+</sup> QPE

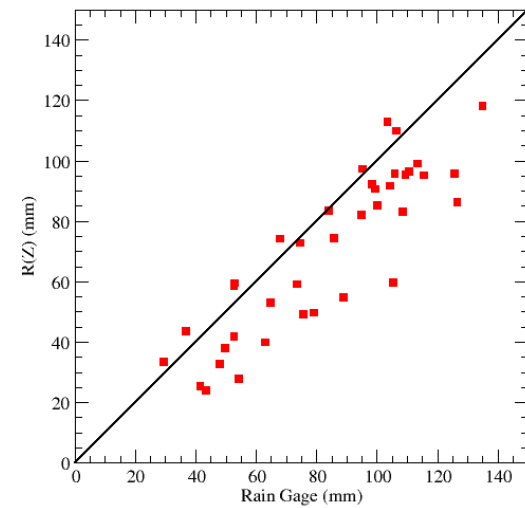


Fig. 11. Three-hour rain totals during the period of the most intense rain measured by gages versus their estimates obtained from the OU PRIME radar using the  $R(Z)$  relation before  $Z$  is corrected for attenuation (upper panel) and after  $Z$  is corrected for attenuation using Eq. (3) (lower panel).

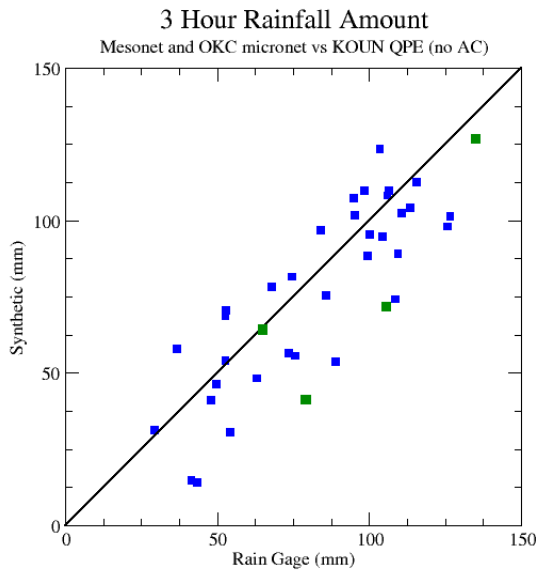


Fig.10. Scatterplot of 3-hour rain totals measured by gages versus their radar estimates using S-band data and the  $R(Z, K_{DP})$  algorithm (2).

The “synthetic” algorithm provides the best accuracy according to all three criteria: fractional bias, fractional standard error, and correlation

### 3 Hour Rainfall Amount

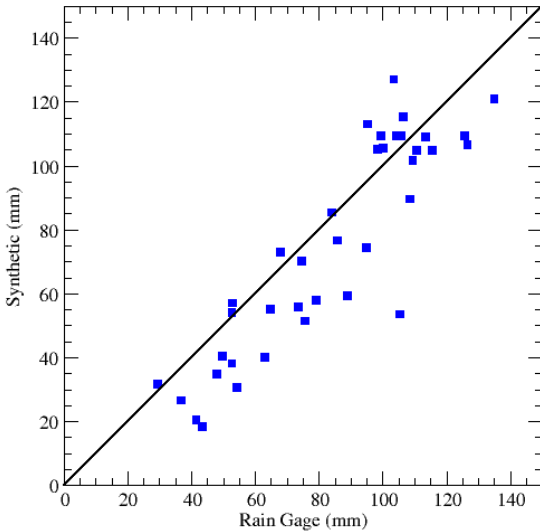


Fig. 12. Same as in Fig. 11 but for the “synthetic” algorithm utilizing Z (corrected for attenuation) in lighter rain and  $K_{DP}$  in heavier rain as prescribed by Eqs. (1) and (4).

Table 2. Quantitative measures of 3-hour rain total radar estimates at C band.

	R(Z) before correction	R(Z) after correction	Synthetic algorithm
Fractional bias	-53.3%	-15.4%	-7.3%
Fractional RMS error	93%	36%	31%
Correlation coefficient	0.76	0.88	0.89

#### 4. FUTURE STUDIES

The most robust polarimetric algorithms at S and C bands heavily rely on the measurements of specific differential phase  $K_{DP}$ . All  $K_{DP}$ -based rainfall products have particular advantage for relatively large spatial / temporal domain (i.e., either for rain accumulations over sufficiently long periods of time or for sufficiently large areas). The fields of instantaneous rain rates retrieved from  $K_{DP}$  may look very noisy and erratic. Moreover, the appearance of negative rain rates is not uncommon, which is very hard to accept for most customers. Generally, the shape and size of individual rain cells can be

distorted in the fields of  $R(K_{DP})$  which is not the case if the  $R(Z)$  or  $R(Z, Z_{DR})$  relations are utilized. This dictates the need to replacing apparently corrupted instantaneous  $R(K_{DP})$  estimates with more robust radar estimates of instantaneous rain. The  $R(Z)$  or  $R(Z, Z_{DR})$  estimates can be utilized as a proxy but they may not be accurate enough in the situations where  $K_{DP}$  has its indisputable advantages (rain mixed with hail, heavy continental rain, or partial beam blockage).

Another possibility to address the problems with  $R(K_{DP})$  is to use rainfall estimate based on specific attenuation  $A$  which can be retrieved via ZPHI method (Testud et al. 2000). Although the ZPHI algorithm was originally introduced at C and X bands, it can be successfully utilized at S band as well, as our recent studies show. The absence of cell distortion and negative rain rates makes the  $R(A)$  estimate a very likely candidate for replacing  $R(K_{DP})$  in the areas where the latter is corrupted.

#### 5. CONCLUSIONS

- Extensive validation study of the rainfall products obtained from the operational KOUN WSR-88D radar during a year period demonstrates that the polarimetric rainfall algorithm based on the joint use of Z and  $K_{DP}$  outperforms the conventional  $R(Z)$  relation for all significant rain events.
- Similar combination of Z and  $K_{DP}$  can be successfully utilized for quantitative estimation of heavy rain at C band as well after radar reflectivity factor is appropriately corrected for attenuation.
- Since the fields of instantaneous rain rates retrieved from  $K_{DP}$  may look noisy and erratic, a possible replacement should be a subject of future investigations.

#### References

Gu, J-Y., A. Ryzhkov, D-I. Lee, B. Wolf, and R. Palmer, 2011: Polarimetric attenuation correction and rainfall estimation for heavy rain events at C band. 35<sup>th</sup> Conf. Radar Meteorol., Pittsburgh, PA.

Palmer, R., D. Bodine, M. Kumjian, B. Cheong, G. Zhang, Q. Cao, H. Bluestein, A. Ryzhkov, T. Yu, Y. Wang, 2011: Observations of the 10 May 2010 tornado outbreak using OU-PRIME: Potential for new science with high-resolution polarimetric radar. *Bulletin of American Meteorological Society*, **92**, 871 – 891.

Testud, J., E. Le Bouar, E. Obligis, and M. Ali-Mehenni, 2000: The rain profiling algorithm applied to polarimetric weather radar. *J. Atmos. Oceanic Technol.*, **17**, 332 – 356.